Acoustic analogs of extremal rotating black holes in exciton-polariton condensates

Anton Svetlichnyi,[1,4] Andrii Chaika,[1] and Alexander Yakimenko[1,2,3]

[1]*Department of Physics, Taras Shevchenko National University of Kyiv, 64/13, Volodymyrska Street, Kyiv 01601, Ukraine*
[2]*Dipartimento di Fisica e Astronomia "Galileo Galilei," Universitá di Padova, via Marzolo 8, 35131 Padua, Italy*
[3]*Istituto Nazionale di Fisica Nucleare, Sezione di Padova, via Marzolo 8, 35131 Padua, Italy*
[4]*Quantum Engineering Centre for Doctoral Training, H. H. Wills Physics Laboratory and Department of Electrical and Electronic Engineering, University of Bristol, Bristol BS8 1FD, United Kingdom*

(Received 16 December 2023; revised 31 March 2024; accepted 18 June 2024; published 26 June 2024)

We theoretically investigate the acoustic analogs of high-angular-momentum rotating black holes in exciton-polariton condensates. Performing numerical simulations of a long-lived ring-shaped condensate configuration with an acoustic horizon and ergoregion for high-angular-momentum states, we observed a quasistable state near critical angular momentum where the acoustic black hole horizon disappears. Our findings offer an insight into the quantum nature of the instability of naked singularity.

DOI: 10.1103/PhysRevB.109.214516

I. INTRODUCTION

Analog physics offers a unique platform for emulating inaccessible phenomena specific to black holes, enabling their study within the controlled environment of laboratory experiments. Following the pioneering work of Unruh [1], numerous approaches have been explored, both theoretically and experimentally, to demonstrate acoustic horizons and analogs of Hawking radiation, including atomic Bose-Einstein condensates (BECs) [2–8], ultracold fermions [9], superfluid ^{3}He [10], trapped ions [11], optical fibers [12–15], electromagnetic waveguides [16], and water tanks [17,18]. A very recent experiment [19] has demonstrated the stabilization of a giant quantum vortex core, hosting thousands of circulation quanta in superfluid ^{4}He. Such a transition of a vortex lattice to the giant vortex in dilute BEC in a superfluid has been theoretically predicted in Ref. [20]. These results open new ways to experimentally explore the analogs of rotating curved spacetimes, offering new perspectives on the interplay between quantum physics and general relativity.

Among the diverse platforms available for studying analog gravity, exciton-polariton condensates stand out as especially promising candidates [21–23]. These condensates offer an ideal experimental setting to emulate sonic black holes with angular momentum, incorporating key features such as the acoustic event horizon and ergoregion, effectively simulating gravitational properties. As was shown by Visser and Weinfurtner [24], although it is not possible to simulate the entire Kerr spacetime in a perfect fluid acoustic form, however, a two-dimensional (2D) equatorial slice of the rotating black hole metric can be realized in analog gravity setups. The exciton-polariton condensate is a very convenient platform for creating 2D black hole analogs: With the ring-shaped pumping the finite lifetime of the polaritons creates a drain in the center of the ring, naturally establishing the density gradient and the radial flow [25,26]. These analogs present a significant opportunity to investigate the intricate quantum properties of black holes, especially those exhibiting high-angular-momentum states [27,28] and study their stability in different dissipative and nondissipative media [29,30]. Moreover, polariton condensates provide the possibility to research the peculiar behavior and configurations of quantum vortices [31,32]. In a recent work [33], Kerr black hole analogs were theoretically investigated and it revealed some remarkable effects, such as the limitation on the angular momentum of the stable system, which resembles a restriction for rotating black holes. General relativity predicts that the angular momentum of the black hole with a given mass has an upper limit defining an extremal black hole. Exceeding this threshold angular momentum, in theory, causes the disappearance of the event horizon, and the appearance of "naked singularity" [34]. To address this theoretical issue, Penrose postulated the cosmic censorship principle [35], which does not allow naked singularities to exist. In particular, in the field of analog black hole physics the authors of a recent work [36] demonstrated that the naked singularities caused by the nondispersive shock waves are prohibited in the atomic BECs. All efforts to theoretically increase a Kerr black hole's angular momentum beyond its maximum limit, aiming to form a naked singularity, have failed. Despite the absence of known counterexamples, cosmic censorship is not yet derived from more fundamental physical concepts, positioning it merely as a hypothesis.

In this paper, we investigate the properties of extremal and superextremal sonic black holes in toroidal exciton-polariton condensates. These intriguing systems suggest an analog to extremal rotating black holes in general relativity, and give rise to important questions concerning their fundamental properties and the mechanisms governing their eventual decay. We demonstrate the stability of acoustic event horizons and ergoregions in a toroidal polariton condensate. We elucidate the mechanisms governing the decay of extremal black holes and the emergence of analogs to naked singularities

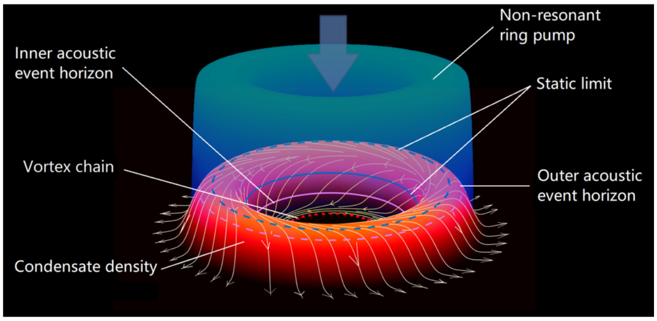

FIG. 1. Schematics of the acoustic analog of rotating black holes in a toroidal exciton-polariton condensate. The blue region is a nonresonant ring pump that creates an exciton-polariton condensate (an orange region). The red-dotted circle is an m-charged vortex chain trapped in the central hole of the toroidal condensate. The magenta lines represent the position of the event horizons, whereas bluish circles represent static limits. Solid lines belong to the inner black hole, whereas dashed lines to the external black hole. The white lines represent the direction of the superflows in the system: From the density peak, they spread inwards and outwards to the internal and external acoustic horizons.

in the exciton-polariton condensate, showing the potentially observable signature of corresponding quantum vortex dynamics. We study the impact of nonequilibrium effects on sonic black hole dynamics, shedding light on the puzzling cosmic censorship principle and the possibility of creating and controlling acoustic analogs of rotating black holes.

II. MODEL

To mimic black hole dynamics in condensed matter systems, it is essential to create an acoustic horizon, analogous to an astrophysical black hole's event horizon. The acoustic horizon divides the regions in the medium, where the flow velocity v_r is higher/lower than the local speed of sound c. Thus, waves generated in the region with $c < v_r$ will propagate radially only in one direction. Additionally, when an astrophysical black hole possesses angular momentum it forms an ergosphere, a region where, due to the frame-dragging effect, no object can remain stationary. To maintain the analogy to a sonic black hole one has to establish the ergoregion in the medium, where the total velocity of the flow is supersound, $v = \sqrt{v_r^2 + v_\varphi^2} > c$, bounded by the static limit ($v = c$).

In the present paper, we consider the system schematically shown in Fig. 1, in which a ring-shaped nonresonant pump creates a condensate with the density gradient on the inner and outer periphery of the ring. Thus, the radial velocity of the condensate v_r can achieve higher values than the speed of sound forming the inner and outer acoustic event horizons, as is seen in Fig. 2. The angular momentum in the system is defined by the number of vortices m, which can be added by the phase imprinting method, which allows for the investigation of the acoustic analogs of rapidly rotating black holes.

The nonresonantly pumped polariton condensate can be described by the mean-field dissipative Gross-Pitaevskii equation (GPE) for the macroscopic wave function ψ coupled to the rate equation for the density of the excitonic reservoir n_R

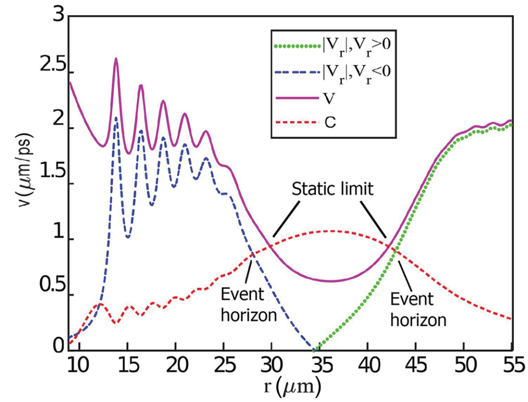

FIG. 2. The radial distribution of the full velocity (magenta line) v and radial component of the velocity (blue line for $v_r < 0$ and green line for $v_r > 0$) of the condensate along with the speed of sound (red line) c. The intersection points of the speed of sound with full and radial velocity are the static limits and acoustic horizons of the black holes, respectively.

(see, e.g., Refs. [37,38]),

$$i\hbar\frac{\partial \psi}{\partial t} = \left[-\frac{\hbar^2}{2M_0}\nabla^2 + g_c|\psi|^2 + g_R n_R + \frac{i\hbar}{2}(R\,n_R - \gamma_c)\right]\psi,$$

$$\frac{\partial n_R}{\partial t} = P(\mathbf{r}, t) - (\gamma_R + R|\psi|^2)n_R, \qquad (1)$$

where $P(\mathbf{r}, t)$ is the optical pumping rate, and g_c and g_R characterize polariton-polariton and polariton-exciton interactions, respectively. The relaxation rates γ_c and γ_R quantify the finite lifetime of condensed polaritons and the reservoir, respectively. The stimulated scattering rate R controls the growth of the condensate density. Note that in comparison with the model employed in Ref. [33] for an analysis of a similar system, our approach involves coupled equations that capture the dynamic evolution of both the condensate wave function and the excitonic reservoir. To achieve a long-lived state with significant angular momentum, we explore various shapes of toroidal pumping $P(\mathbf{r}, t)$.

III. LONG-LIVED CONFIGURATION OF THE BLACK HOLE

To explore the analog of a rotating black hole, we establish an acoustic analog of the static limit and the event horizon. The static limit arises when the Bogoliubov speed of sound, given by $c = \sqrt{g_c|\Psi|^2/M_0}$, matches the full velocity of the condensate, denoted as $\mathbf{v} = (\hbar/M_0)\nabla \arg(\Psi)$. The existence of an acoustic horizon occurs in the region where $c = v_r$, with v_r representing the radial velocity of the condensate. Creating a long-lived analog of a black hole in polariton condensates requires a radially symmetric pump that effectively drains polaritons in the near-center region of the toroidal condensate. The essential properties of sonic black holes are governed by the condensate density gradient which can be tuned by the shape of the pump. In this paper, we employed two types of pumping to achieve long-lived states with high angular momentum. First, we consider a simple ring-shaped pump,

$$P = P_0 \ \exp\left\{-\left(\frac{r - r_0}{w}\right)^4\right\}, \tag{2}$$

where $P_0 = 65\ \mu\mathrm{m}^{-1}\ \mathrm{ps}^{-1}$ is the optical pumping amplitude, and $r_0 = 36\ \mu\mathrm{m}$, $w = 10\ \mu\mathrm{m}$ controls the width of the ring. First of all, we created the stable nonextremal rotating black hole with $m = 19$, to study the properties of this peculiar system. Due to the ring topology of the pump, there are two acoustic horizons and static limits in the system: on the outer and inner periphery of the ring (Fig. 2). Consequently, we call the part of the system, where the radial velocity of the condensate is directed toward the center, as the inner black hole region, and the outer black hole if the radial flow is directed outward to the external periphery. But the distance between the outer static limit and the horizon is too small ($\approx 1\ \mu\mathrm{m}$) so it becomes hard to study the properties of the ergosphere in that case. That is why we concentrate our studies on the black hole on the inner periphery, where the analogy to the real black holes can be explored more precisely.

It is worth mentioning that the long-term evolution of the condensate does not depend on initial conditions, due to the strongly dissipative nature of the exciton-polariton condensate, with the short lifetime of the polaritons $\tau_p \approx 3$ ps. To observe the long-lived solution as in Fig. 2, typically of the order of 50 ps was sufficient for the currents to stabilize, starting from the initial random noise with imprinted vortices in the center of the future ring. Moreover, in our simulations, the final state after a relaxation was mainly insensitive to the position of the vortex imprinting inside the acoustic horizon. In addition, we numerically verified that such states can live at least 10^3 ps. Therefore we consider stable evolution for times $t > 100$ ps, as long-lived dynamics. Note that experimentally accessible time resolution allows the observation of the vortex dynamics at timescales of order 10 ps [39,40].

A. Bessel modes

There are several very peculiar properties in that system. First is the standing wave (set of density circles) inside the inner black hole region [Fig. 3(b)], similar to what was observed in Ref. [41]. This effect is connected with polariton creation and decay in the low-density region and it is solely the property of the exciton-polariton condensate. This effect can be explained in terms of the low-density approximation.

We are searching for stationary solutions of the system in the form of a standard ansatz,

$$\psi(r, t) = \Psi(r)e^{-i\mu t/\hbar},$$
$$n_R(r) = \frac{P(r)}{\gamma_r + R|\Psi|^2}. \tag{3}$$

Due to the absence of a pump in the decaying region, we can neglect pumping and nonlinear terms in Eq. (1). This approximation gives us

$$\mu\Psi = \left(-\frac{\hbar^2}{2M_0}\nabla^2 - \frac{i\hbar}{2}\gamma_c\right)\Psi. \tag{4}$$

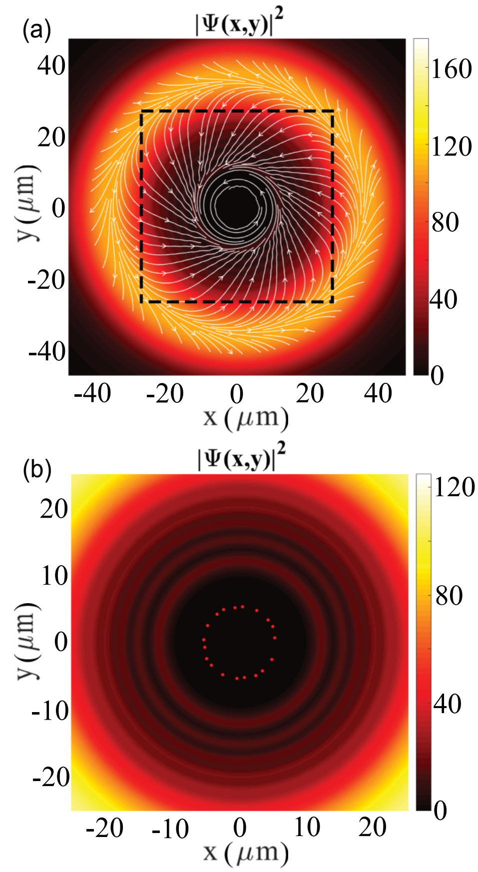

FIG. 3. (a) Density of states for the stable configuration ($m = 19$) along with contour lines of the total velocity (white lines) of the condensate. (b) Bessel modes inside the highlighted region of (a). Red points denote vortices.

This is the well-known Helmholtz equation. In the central decaying region solution which can be written in terms of Bessel functions of the first kind,

$$\Psi(r) \sim J_m(kr)e^{im\phi}. \tag{5}$$

Consequently, for the outer black hole region, we can write the solution in the form of Hankel functions of the first kind,

$$\Psi(r) \sim H_m^1(kr)e^{im\phi} \approx \frac{e^{i(kr+m\phi)}}{\sqrt{kr}}, \tag{6}$$

where $k = \sqrt{\widetilde{\mu} + iM_0\gamma_c/\hbar}$ and $\widetilde{\mu} = 2M_0\mu/\hbar^2$. Here, the wave number exhibits a complex argument, however, in our simulations, the imaginary part is usually 15–30 times smaller than the absolute value. Consequently, within the low-density region, the wave function demonstrates behavior closely resembling that of a Bessel function with a real argument (see Fig. 3).

It is worth mentioning that the imaginary part of k yields the nonzero radial velocity. The comparison between the theoretical estimation and results of the simulations is presented in Fig. 4(a). One can see a good agreement between the radial velocity of the condensate and the speed of sound inside the low-density region. The divergences are caused by the influence of the pumping and nonlinear effects.

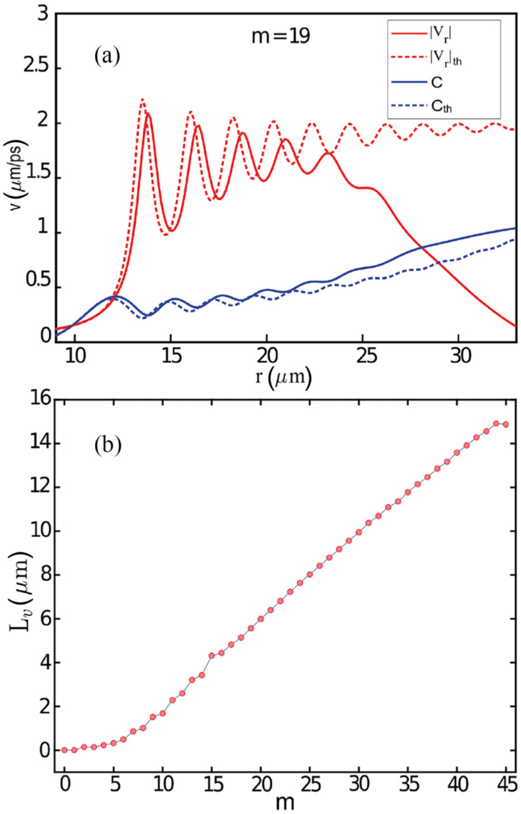

FIG. 4. (a) A comparison of the approximate estimate for the speed of sound (dashed blue line) and radial velocity (dashed red line) with the results of the numerical simulations (solid red and blue lines, correspondingly). (b) The vortex chain radius L vs the topological charge m for the pumping shape given by Eq. (2).

B. Critical angular momentum of the black hole

One of the most remarkable features of the ring-shaped exciton-polariton condensates is the formation of the vortex chain, seen in Fig. 3(b), which has been experimentally observed before in a resonantly pumped polariton superfluid [42]. The radius of the vortex chain increases linearly with topological charge [see Fig. 4(b)], which leads to the decay of the persistent current above some critical value of the angular momentum.

As mentioned above, we concentrate our studies on the inner black hole region with the flow directed to the center of the ring, i.e., with *negative* radial velocity. From Eq. (1) one can obtain the following continuity equation for the stationary state Eq. (3),

$$\nabla(\rho\vec{v}) = \rho\left(-\gamma_c + \frac{PR}{\gamma_R + R\rho}\right). \tag{7}$$

On the right-hand side of (7) are the "source" and "sink" terms of the condensate. We call the line at which the right-hand side vanishes the gain-loss border. Also for convenience, we call the line at which radial velocity changes the sign ($v_r = 0$) "the watershed." Integrating (7) over the inner black hole region, up to the watershed, and applying the divergence theorem,

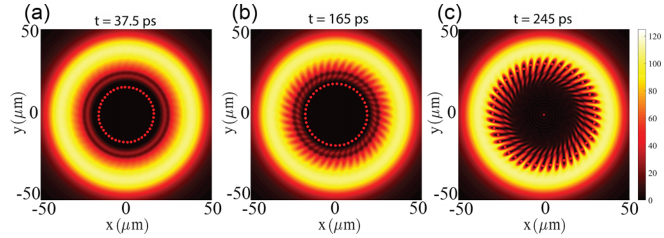

FIG. 5. Density $|\psi|^2$ for the pump (2) illustrating unstable system evolution with $m = 44$ at different times. The red points denote vortex core positions.

we get

$$\int \rho\left(-\gamma_c + \frac{PR}{\gamma_R + R\rho}\right)dS = 0. \tag{8}$$

That expression describes the balance of the flow generation in the sink and source regions. When the system gains additional angular momentum the condensate is forced out from the center by centrifugal force, and the density in the sink region is decreasing faster than in the source region. To fulfill the balance, in (8), the area of the source part must decrease, so the watershed shifts closer to the axis of the ring.

At high angular momentum, due to the proximity to the vortex chain, the density near the gain-loss border is negligible, and the radial coordinate r_* of the critical gain-loss border can be obtained from the following equation,

$$P(r_*) = \frac{\gamma_c\gamma_R}{R}. \tag{9}$$

Thus theoretically vortex chain radius cannot exceed r_*, to fulfill the continuity equation for a stationary state. Indeed, our simulations reveal that when the vortex chain approaches the gain-loss boundary, the radial velocity of the condensate turns unidirectional, leading to the disappearance of the inner black hole's acoustic horizon—a behavior analogous to a naked singularity in general relativity. By unidirectional flows, we mean here that all flows in regions with a significant condensate density have a positive radial projection, thus flowing out of the system. However, in practice, vortices exiting the condensate typically prevent this state, as illustrated in Fig. 5. Specifically, with the pump (2), our simulations demonstrate a maximum angular momentum of $m = 43$ and a vortex chain radius of $L = 15.8$ μm, which is less than the critical gain-loss border, $r_* = 25.2$ μm, hence vortices start leaving the condensate before the event horizon disappears.

C. High-angular-momentum state

In our studies, we tested several pumps to create a black hole analog. To demonstrate the disappearance of the horizon above some threshold angular momentum, we introduced the following ring-shaped pump, which is similar to the stable pump, studied in Ref. [43],

$$P = P_0\left(1 - \exp\left\{-\left(\frac{r}{w}\right)^4\right\}\right)\exp\left\{-\left(\frac{r}{w}\right)^8\right\}, \tag{10}$$

where $P_0 = 170$ μm^{-1} ps^{-1} is the optical pumping amplitude, and $w = 56$ μm is the width of the ring. At low momentum

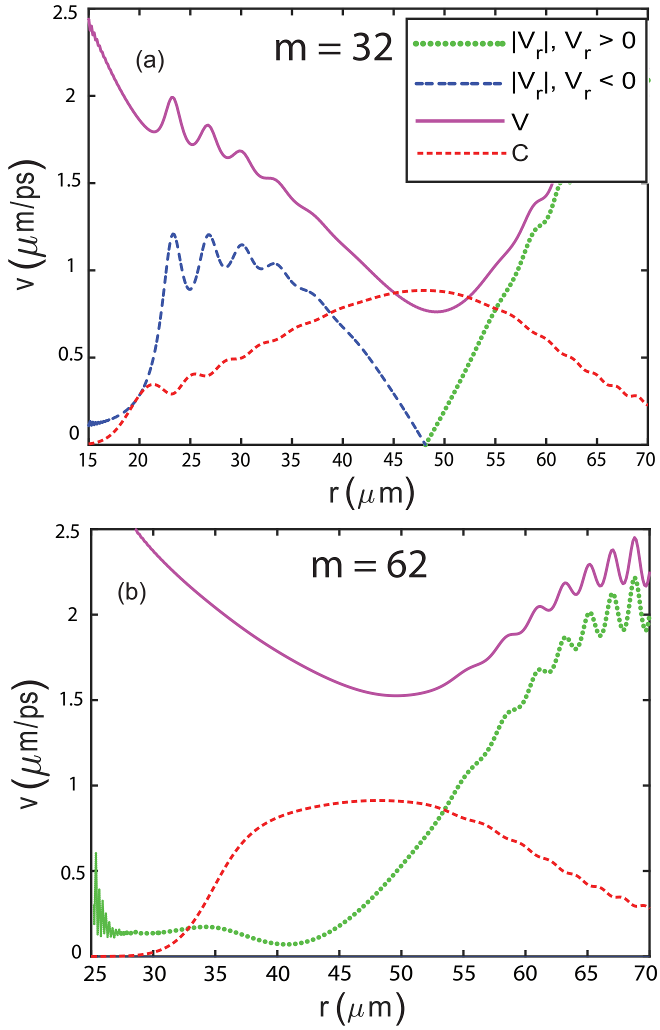

FIG. 6. The velocity of the condensate and speed of sound dynamics for pump (10): (a) $m = 32$, long-lived state. (b) $m = 62$, the state with unidirectional flows—complete disappearance of the inner event horizon.

($m = 32$), we observe a robust acoustic analog of a rotating black hole [Fig. 6(a)]. To further enhance the system's angular momentum, we systematically introduce five vortices at the center of the ring with a time interval of 30 ps (Fig. 7).

As noted, as the ring-shaped vortex chain expands toward the horizon, the area between the horizon and vortex cores diminishes [Fig. 6(b)]. A noteworthy phenomenon occurs when the vortex chain meets the acoustic horizon: The black hole horizon vanishes, resulting in a unidirectional flow towards the outer periphery [Fig. 8(a)]. As each vortex contains the phase singularity and the vortex chain radius is proportional to the angular momentum of the system, a ring-shaped vortex chain can be analogously interpreted as a representation of a ring-shaped singularity in the Kerr black hole, the radius of which is also proportional to the angular momentum of the black hole [44]. Therefore this state with unidirectional flow can be treated as an analog of a superextremal black hole with a naked singularity.

In our simulations, we observed that state with a vortex chain radius of less than the critical gain-loss border

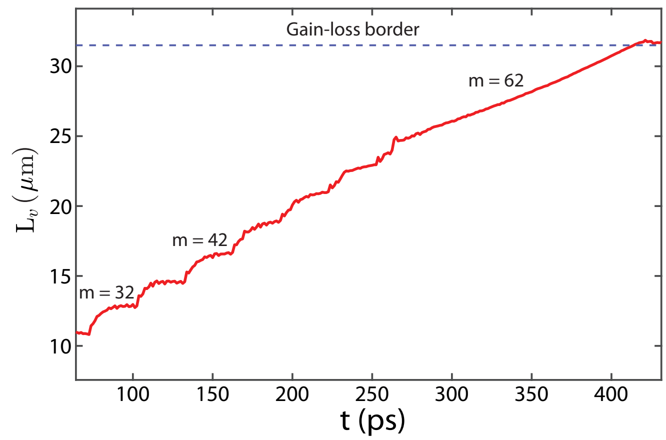

FIG. 7. The time-dependent radius of the vortex chain (red line) and the critical gain-loss border (blue dashed line). We imprint five vortices every 30 ps until radial flows become unidirectional ($m = 62$). Upon reaching the gain-loss boundary, the ring-shaped vortex chain decays, and vortex lines escape the condensate.

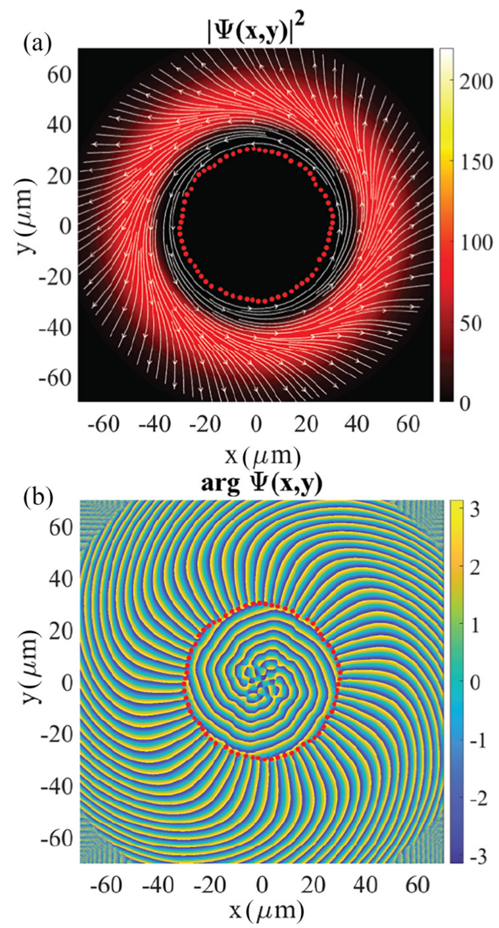

FIG. 8. (a) Density $|\Psi|^2$ with overlaid streamlines representing the condensate flow (white lines with arrows), notably transitioning into a unidirectional state. (b) Condensate phase, highlighting the ring-shaped vortex chain. Positions of the vortex cores are indicated by red points.

$r_* = 31.5$ μm due to the finite size of the vortices, which is not taken into account in Eq. (8). The divergence is an order of the characteristic length between the vortices ≈ 2.5 μm.

It is important to highlight that the current state of the system is metastable, and characterized by a limited lifetime. As illustrated in Fig. 7, the radius of the vortex chain grows throughout 100 ps. Subsequently, beyond this time frame, vortices begin leaving the condensate. Note that the number of vortices in the vortex chain on Fig. 8 is equal to 68, not 62 as the total topological charge of the system. Inside the low-density region, there is a constant process of vortex-antivortex pair annihilation and creation. Due to the noisy phase in the center of the system, we decided not to depict these vortices and antivortices in Fig. 8. The extra six vortices in the vortex chain are connected with the corresponding antivortices inside the central low-density region of the toroidal condensate, so the full topological charge is conserved.

IV. CONCLUSIONS

We investigated acoustic analogs of rotating black hole event horizons formed by the persistent currents in the ring-shaped exciton-polariton condensate with two acoustic event horizons formed by the radial superflows of the condensate. We have found that above a critical angular momentum threshold, a reversal in radial flow occurred. Intriguingly, this transition coincided with the disappearance of the internal acoustic event horizon resembling a hypothetical superextremal black hole. However, such a scenario is unlikely to occur in nature, as superextremal black holes are unstable and would quickly lose angular momentum through radiation or accretion. Theoretically predicted in our work, a long-lived transitory state can be treated as an acoustic analog of a black hole with *naked singularity*. These unusual states finally decay so that the "cosmic censorship principle" appears to be fulfilled for the stable stationary states.

Our findings hold promise for a profound exploration of the quantum properties of Kerr black holes using acoustic analogs within well-controlled laboratory environments of exciton-polariton condensates.

ACKNOWLEDGMENTS

We acknowledge L. Salasnich and E. Ostrovskaya for useful discussions. The authors acknowledge support from the National Research Foundation of Ukraine through Grant No. 2020.02/0032. A.Y. acknowledges support from the BIRD Project Ultracold atoms in curved geometries of the University of Padova. A.S. acknowledges the support from the Engineering and Physical Sciences Research Council (EP/SO23607/1) via the Centre for Doctoral Training at the University of Bristol.

[1] W. G. Unruh, Experimental black-hole evaporation? Phys. Rev. Lett. **46**, 1351 (1981).

[2] I. Carusotto, S. Fagnocchi, A. Recati, R. Balbinot, and A. Fabbri, Numerical observation of Hawking radiation from acoustic black holes in atomic Bose Einstein condensates, New J. Phys. **10**, 103001 (2008).

[3] C. Mayoral, A. Recati, A. Fabbri, R. Parentani, R. Balbinot, and I. Carusotto, Acoustic white holes in flowing atomic Bose-Einstein condensates, New J. Phys. **13**, 025007 (2011).

[4] O. Lahav, A. Itah, A. Blumkin, C. Gordon, S. Rinott, A. Zayats, and J. Steinhauer, Realization of a sonic black hole analog in a Bose-Einstein condensate, Phys. Rev. Lett. **105**, 240401 (2010).

[5] J. Steinhauer, Observation of quantum Hawking radiation and its entanglement in an analogue black hole, Nat. Phys. **12**, 959 (2016).

[6] J. R. Muñoz de Nova, K. Golubkov, V. I. Kolobov, and J. Steinhauer, Observation of thermal Hawking radiation and its temperature in an analogue black hole, Nature (London) **569**, 688 (2019).

[7] A. Fabbri and R. Balbinot, Ramp-up of Hawking radiation in Bose-Einstein-condensate analog black holes, Phys. Rev. Lett. **126**, 111301 (2021).

[8] I. Yatsuta, B. Malomed, and A. Yakimenko, Acoustic analog of Hawking radiation in quantized circular superflows of Bose-Einstein condensates, Phys. Rev. Res. **2**, 043065 (2020).

[9] S. Giovanazzi, Hawking radiation in sonic black holes, Phys. Rev. Lett. **94**, 061302 (2005).

[10] T. A. Jacobson and G. E. Volovik, Event horizons and ergoregions in ^{3}He, Phys. Rev. D **58**, 064021 (1998).

[11] B. Horstmann, B. Reznik, S. Fagnocchi, and J. I. Cirac, Hawking radiation from an acoustic black hole on an ion ring, Phys. Rev. Lett. **104**, 250403 (2010).

[12] T. G. Philbin, C. Kuklewicz, S. Robertson, S. Hill, F. König, and U. Leonhardt, Fiber-optical analog of the event horizon, Science **319**, 1367 (2008).

[13] F. Belgiorno, S. L. Cacciatori, M. Clerici, V. Gorini, G. Ortenzi, L. Rizzi, E. Rubino, V. G. Sala, and D. Faccio, Hawking radiation from ultrashort laser pulse filaments, Phys. Rev. Lett. **105**, 203901 (2010).

[14] W. G. Unruh and R. Schützhold, Hawking radiation from "phase horizons" in laser filaments? Phys. Rev. D **86**, 064006 (2012).

[15] S. Liberati, A. Prain, and M. Visser, Quantum vacuum radiation in optical glass, Phys. Rev. D **85**, 084014 (2012).

[16] R. Schützhold and W. G. Unruh, Hawking radiation in an electromagnetic waveguide? Phys. Rev. Lett. **95**, 031301 (2005).

[17] S. Weinfurtner, E. W. Tedford, M. C. J. Penrice, W. G. Unruh, and G. A. Lawrence, Measurement of stimulated Hawking emission in an analogue system, Phys. Rev. Lett. **106**, 021302 (2011).

[18] G. Rousseaux, C. Mathis, P. Maïssa, T. G. Philbin, and U. Leonhardt, Observation of negative-frequency waves in a water tank: A classical analogue to the Hawking effect? New J. Phys. **10**, 053015 (2008).

[19] P. Švančara, P. Smaniotto, L. Solidoro, J. F. MacDonald, S. Patrick, R. Gregory, C. F. Barenghi, and S. Weinfurtner, Rotating curved spacetime signatures from a giant quantum vortex, Nature **628**, 66 (2024).

[20] U. R. Fischer and G. Baym, Vortex states of rapidly rotating dilute Bose-Einstein condensates, Phys. Rev. Lett. **90**, 140402 (2003).

[21] D. D. Solnyshkov, H. Flayac, and G. Malpuech, Black holes and wormholes in spinor polariton condensates, Phys. Rev. B **84**, 233405 (2011).

[22] M. Jacquet, M. Joly, F. Claude, L. Giacomelli, Q. Glorieux, A. Bramati, I. Carusotto, and E. Giacobino, Analogue quantum simulation of the Hawking effect in a polariton superfluid, Eur. Phys. J. D **76**, 152 (2022).

[23] H. S. Nguyen, D. Gerace, I. Carusotto, D. Sanvitto, E. Galopin, A. Lemaître, I. Sagnes, J. Bloch, and A. Amo, Acoustic black hole in a stationary hydrodynamic flow of microcavity polaritons, Phys. Rev. Lett. **114**, 036402 (2015).

[24] M. Visser and S. Weinfurtner, Vortex analogue for the equatorial geometry of the Kerr black hole, Class. Quantum Grav. **22**, 2493 (2005).

[25] M. Jacquet, T. Boulier, F. Claude, A. Matre, E. Cancellieri, C. Adrados, A. Amo, S. Pigeon, Q. Glorieux, and E. Giacobino, Polariton fluids for analogue gravity physics, Philos. Trans. R. Soc. A **378**, 20190225 (2020).

[26] C. Barceló, Analogue black-hole horizons, Nat. Phys. **15**, 210 (2019).

[27] S.-D. Jheng, T.-W. Chen, and S.-C. Cheng, Spontaneous giant vortices and circular supercurrents in a trapped exciton-polariton condensate, Opt. Express **30**, 35325 (2022).

[28] S. N. Alperin and N. G. Berloff, Multiply charged vortex states of polariton condensates, Optica **8**, 301 (2021).

[29] S. Patrick, A. Geelmuyden, S. Erne, C. F. Barenghi, and S. Weinfurtner, Quantum vortex instability and black hole superradiance, Phys. Rev. Res. **4**, 033117 (2022).

[30] T. A. S. Cardoso and M. Richartz, Dissipative quantum vortices and superradiant scattering, Phys. Rev. A **106**, 063310 (2022).

[31] J. Keeling and N. G. Berloff, Spontaneous rotating vortex lattices in a pumped decaying condensate, Phys. Rev. Lett. **100**, 250401 (2008).

[32] T. Cookson, K. Kalinin, H. Sigurdsson, J. D. Töpfer, S. Alyatkin, M. Silva, W. Langbein, N. G. Berloff, and P. G. Lagoudakis, Geometric frustration in polygons of polariton condensates creating vortices of varying topological charge, Nat. Commun. **12**, 2120 (2021).

[33] D. D. Solnyshkov, C. Leblanc, S. V. Koniakhin, O. Bleu, and G. Malpuech, Quantum analogue of a Kerr black hole and the Penrose effect in a Bose-Einstein condensate, Phys. Rev. B **99**, 214511 (2019).

[34] R. P. Kerr, Gravitational field of a spinning mass as an example of algebraically special metrics, Phys. Rev. Lett. **11**, 237 (1963).

[35] R. Penrose, Gravitational collapse: The role of general relativity, Riv. Nuovo Cimento **1**, 252 (1969).

[36] U. R. Fischer and S. Datta, Dispersive censor of acoustic spacetimes with a shock-wave singularity, Phys. Rev. D **107**, 084023 (2023).

[37] M. Wouters and I. Carusotto, Excitations in a nonequilibrium Bose-Einstein condensate of exciton polaritons, Phys. Rev. Lett. **99**, 140402 (2007).

[38] G. Li, M. D. Fraser, A. Yakimenko, and E. A. Ostrovskaya, Stability of persistent currents in open dissipative quantum fluids, Phys. Rev. B **91**, 184518 (2015).

[39] D. Sanvitto, F. M. Marchetti, M. H. Szymańska, G. Tosi, M. Baudisch, F. P. Laussy, D. N. Krizhanovskii, M. S. Skolnick, L. Marrucci, A. Lemaître, J. Bloch, C. Tejedor, and L. Viña, Persistent currents and quantized vortices in a polariton superfluid, Nat. Phys. **6**, 527 (2010).

[40] B. Deveaud, Exciton-polariton Bose-Einstein condensates, Annu. Rev. Condens. Matter Phys. **6**, 155 (2015).

[41] X. Ma and S. Schumacher, Vortex multistability and Bessel vortices in polariton condensates, Phys. Rev. Lett. **121**, 227404 (2018).

[42] T. Boulier, H. Terças, D. D. Solnyshkov, Q. Glorieux, E. Giacobino, G. Malpuech, and A. Bramati, Vortex chain in a resonantly pumped polariton superfluid, Sci. Rep. **5**, 9230 (2015).

[43] X. Ma, U. Peschel, and O. A. Egorov, Incoherent control of topological charges in nonequilibrium polariton condensates, Phys. Rev. B **93**, 035315 (2016).

[44] S. A. Teukolsky, The Kerr metric, Class. Quantum Grav. **32**, 124006 (2015).